Hindawi Publishing Corporation
Advances in Materials Science and Engineering
Volume 2013, Article ID 974507, 6 pages
http://dx.doi.org/10.1155/2013/974507

Research Article

Effects of the Boron-Doped p^+ Emitter on the Efficiency of the n-Type Silicon Solar Cell

Eun-Young Kim and Jeong Kim

Department of Electronics Engineering, Sejong University, Seoul 143-747, Republic of Korea

Correspondence should be addressed to Jeong Kim; kimjeong@sejong.ac.kr

Received 26 July 2013; Accepted 13 September 2013

Academic Editor: Seung Hwan Ko

The optimum structure of the p^+ emitter for the n-type silicon solar cell was determined with the simulation of the boron doping concentration. The boron concentration (N_B) in the p^+ emitter was varied in the range of 1×10^{17} and 2×10^{22} atoms/cm^3 while maintaining the base doping concentration at 2×10^{16} atoms/cm^3. With the increase of the boron concentration, the open circuit voltage (V_{OC}) of the cell increased up to 0.525 V and then was nearly saturated at $N_B > 5 \times 10^{18}$ atoms/cm^3. On the other hand, the short circuit current density (J_{SC}) began to decrease at $N_B > 1 \times 10^{19}$ atoms/cm^3 due to the increase of the surface recombination loss, and without considering the variation of the contact resistance along the emitter doping level, the maximum efficiency of the cell was obtained at around $N_B = 5 \times 10^{18}$ atoms/cm^3. While the contact resistance of the electrode decreases with the increase of the doping concentration in the p^+ emitter, and with consideration of the variation of the contact resistance, the optimum value of N_B for maximum efficiency shifted to the higher doping level.

1. Introduction

Currently, the p-type silicon solar cell comprises a large portion of the industrial solar cells. On the other hand, the n-type silicon solar cell has been known to have many advantages and has subsequently received a great deal of attention and has become one of the main development topics in PV industries. Crystalline silicon solar cell using the n-type wafer showed the highest efficiency record among commercial silicon solar cells [1]. The n-type wafer has a longer diffusion length than the p-type wafer as a result of a higher tolerance to common transition metal impurities [2, 3]. Also, it does not contain any boron-oxide pairs, which are considered as the origin of light-induced degradation (LID) in the p-type Si wafer [4]. Thus, the performance of the n-type silicon solar cell can almost be maintained without degradation during the illumination of light. Furthermore, since the doping profile of boron is more similar to the theoretical model than that of phosphorous, the application of simulation to the real emitter diffusion process is more suitable for the n-type Si wafer.

In spite of the definite advantages of n-type silicon, p-type silicon comprises 85% of industrial silicon solar cells. Historically, research and process infrastructure have been mainly developed for p-type silicon solar cells, which are essential to make economical and high-efficient commercial solar cells.

In order to realize a p^+ emitter on n-type silicon wafer, three kinds of methods are usually applied: (i) boron-diffused emitter, (ii) Al-alloyed emitter, and (iii) heterojunction using p-type a-Si [5]. Among these methods, the boron-diffused emitter is most similar to the phosphorus-diffused emitter of the conventional p^+ silicon solar cell. But, in the case of the diffusion of boron, a noticeable gettering effect was not shown compared with the diffusion of phosphorus. And BSG (boron silicate glass), which is formed during boron diffusion [6, 7], is not completely removed by chemical solution (usually HF), while it is easy to remove PSG (phosphorus silicate glass) using HF solution.

In this study, the structure of the p^+ emitter doped with boron was optimized for the n-type silicon solar cell. The performance of the solar cell was simulated varying

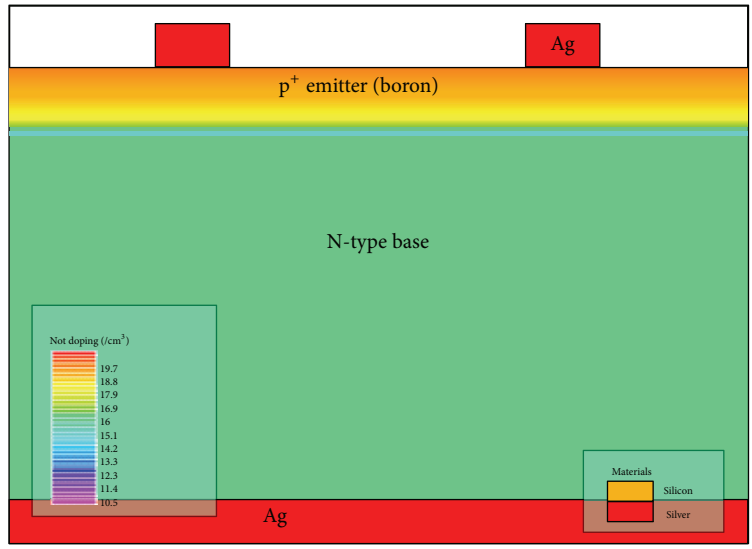

FIGURE 1: Schematic cross-section of boron-doped p^+ emitter for n-type silicon solar cell.

the contact resistance (R_C) of the electrode and the doping concentration of boron.

2. Simulation Scheme

The Silvaco TCAD tool, which is commonly used for the simulation of semiconductor devices, was used to simulate and optimize the emitter structure for the n-type silicon solar cell. During the simulation, an n-type crystalline silicon wafer with an orientation of (100) was chosen and the base doping concentration of phosphorus was set to 1×10^{16} atoms/cm^3. The p^+ emitter was formed diffusing the boron into the silicon at 900°C for 10 min varying the boron concentration [8], and silver was used for electrode materials on the front and rear surfaces. Figure 1 shows the structure of the n-type silicon solar cell used in this simulation.

The width and the height of the simulation region in Figure 1 were 120 and 1200 μm, respectively, and the default depth of the simulation region was 1 μm. The centers of the front electrodes with widths of 100 μm were spaced out 600 μm apart.

The diffusion models describe how dopants and defects in the silicon redistribute themselves during thermal treatment, due to concentration gradients and internal electric fields. When modeling the actual diffusion process, there are additional effects to consider such as impurity clustering, activation, and how interfaces are treated [9]. In this study, the diffusion of the boron was simulated using the advanced diffusion model developed at CNRS-Phase (Strasbourg, France), CEA-LETI (Grenoble, France), and Silvaco [10]. Basically, the dopants and the point defects move in the silicon along the following diffusion equation [10]:

$$\frac{\partial C_{\text{tot}}}{\partial t} = -\nabla J_A + S, \tag{1}$$

where C_{tot} is the total impurity concentration, S is the source and sink terms, and J_A is the flux of mobile particle as

$$J_A = -D_A \nabla C_A + C_A \mu E. \tag{2}$$

In the above equation, C_A is the mobile impurity concentration, D_A is the diffusivity of the impurity, μ is the mobility, and E is the electric field.

Generally, the shallow emitter shows low surface recombination and good blue response at the short wavelength region, but the metal contact on the front surface is ready to show high resistance. To decrease the contact resistance, the emitter should be doped heavily with the doping materials [11]. Firstly, assuming the contact resistance, R_C, as zero, the boron concentration, N_B, in the p^+ emitter was varied in the range of 1×10^{17}–2×10^{22} atoms/cm^3. In the second simulation, the contact resistance was varied in the range of 0–0.5 Ωcm^2, fixing the concentration of boron at 5×10^{18} atoms/cm^3. Finally, two parameters, N_B and R_C, were simultaneously considered, and the output parameters of the cell were compared with the former results.

3. Results and Discussion

3.1. Dependence of the Cell Parameters on N_B. Figure 2 shows the dependence of the output parameters of the cell on the boron concentration, N_B. The N_B in the p^+ emitter was varied in the range of 1×10^{17}–2×10^{22} atoms/cm^3, and the contact resistance was assumed to be zero. With the increase of N_B, the open circuit voltage, V_{OC}, of the cell increased as well and saturated at $N_B > 5 \times 10^{18}$ atoms/cm^3. Meanwhile, the short circuit current density, J_{SC}, began to decrease at $N_B > 1 \times 10^{19}$ atoms/cm^3. The increase of the doping concentration in the p^+ emitter may cause an increase in the carrier density and a decrease of the quasi-fermi level of the hole, which resulted in the increase of the V_{OC}. However, since heavy doping can also bring about an increase in recombination loss in

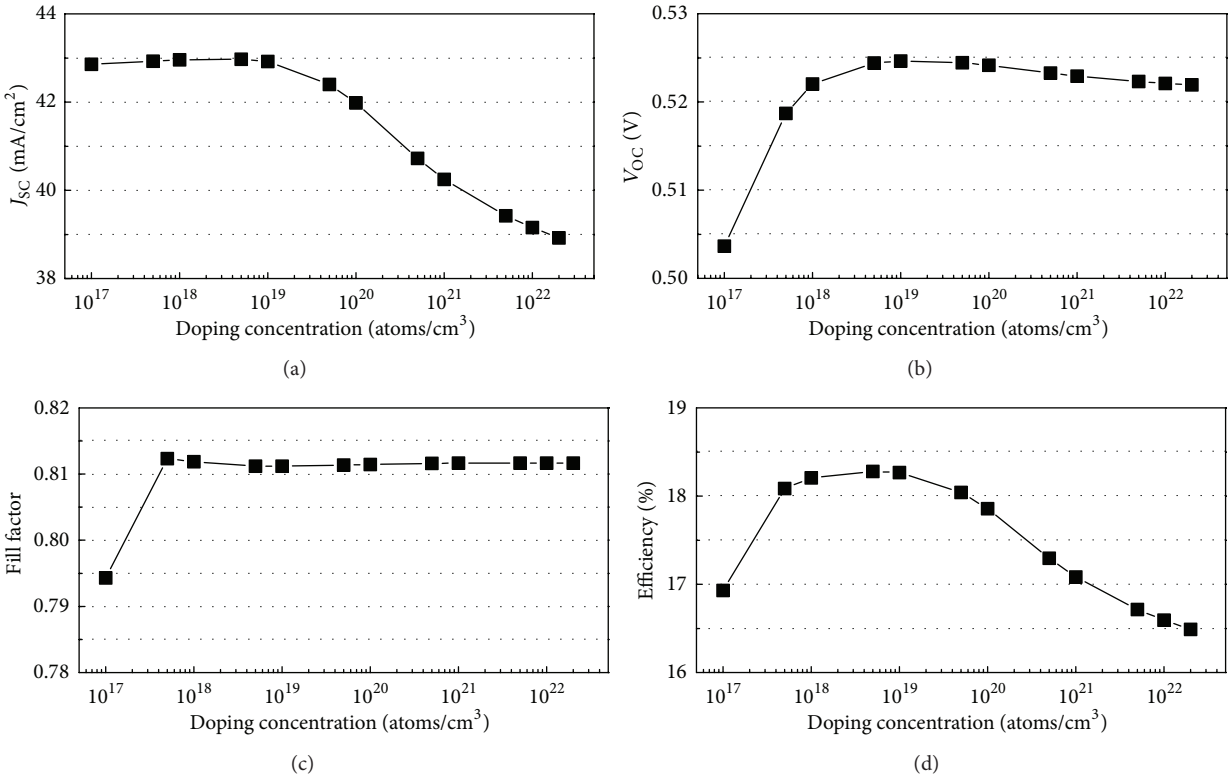

FIGURE 2: Dependence of the output parameters: (a) short circuit current density, (b) open circuit voltage, (c) fill factor, and (d) efficiency of the cell, on the boron concentration.

the emitter region, V_{OC} was saturated at $N_B > 5 \times 10^{18}$ atoms/cm^3. Also, the increase of recombination loss of the light-induced carrier meant the decrease of J_{SC} at $N_B > 1 \times 10^{19}$ atoms/cm^3. Consequently, the efficiency of the cell showed a maximum value of $N_B = 5 \times 10^{18}$–1×10^{19} atoms/cm^3.

In order to confirm the recombination loss in the emitter region for the high doping concentration of boron, internal quantum efficiency (IQE) of the cell was calculated along the N_B as shown in Figure 3. In the short wavelength range, IQE rapidly decreased at $N_B > 1 \times 10^{19}$ atoms/cm^3, while there was no significant difference in the long wavelength range. This means that the recombination loss occurred at the front emitter region and is closely related to the decrease of the J_{SC}, as mentioned above.

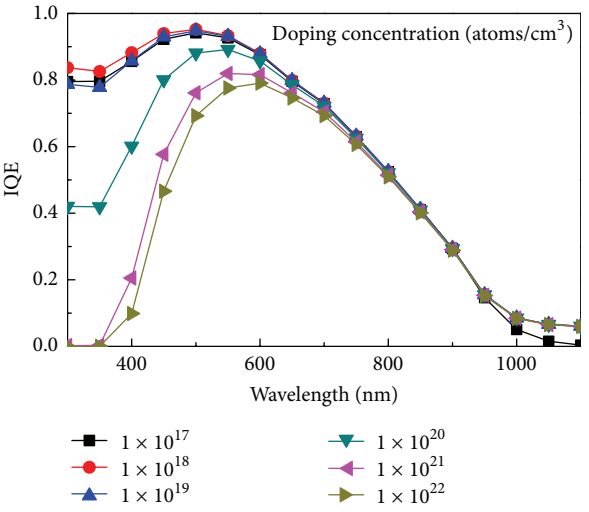

FIGURE 3: Variation of the internal quantum efficiency of the cell with different boron concentration.

3.2. Effect of the Contact Resistance. Though the surface recombination loss increases with the increase of N_B, conventional cell generally employs a heavily doped emitter that provides low contact resistance of the front electrode. On the other hand, the shallow emitter shows a low surface recombination loss and a good blue response of the cell at the short wavelength region, but a high contact resistance.

Figure 4 shows the output parameters of the cell along the contact resistance of the front electrode fixing the boron concentration at 5×10^{18} atoms/cm^3 in the emitter region. The fill factor of the cell was most affected by the contact resistance, as expected. J_{SC} and V_{OC} were slightly dependent on the contact resistance in such a way that J_{SC} decreased but V_{OC} increased with the increase of the contact resistance. The behavior of V_{OC} could be understood from the decrease of the remanent carrier concentration in the emitter region for low

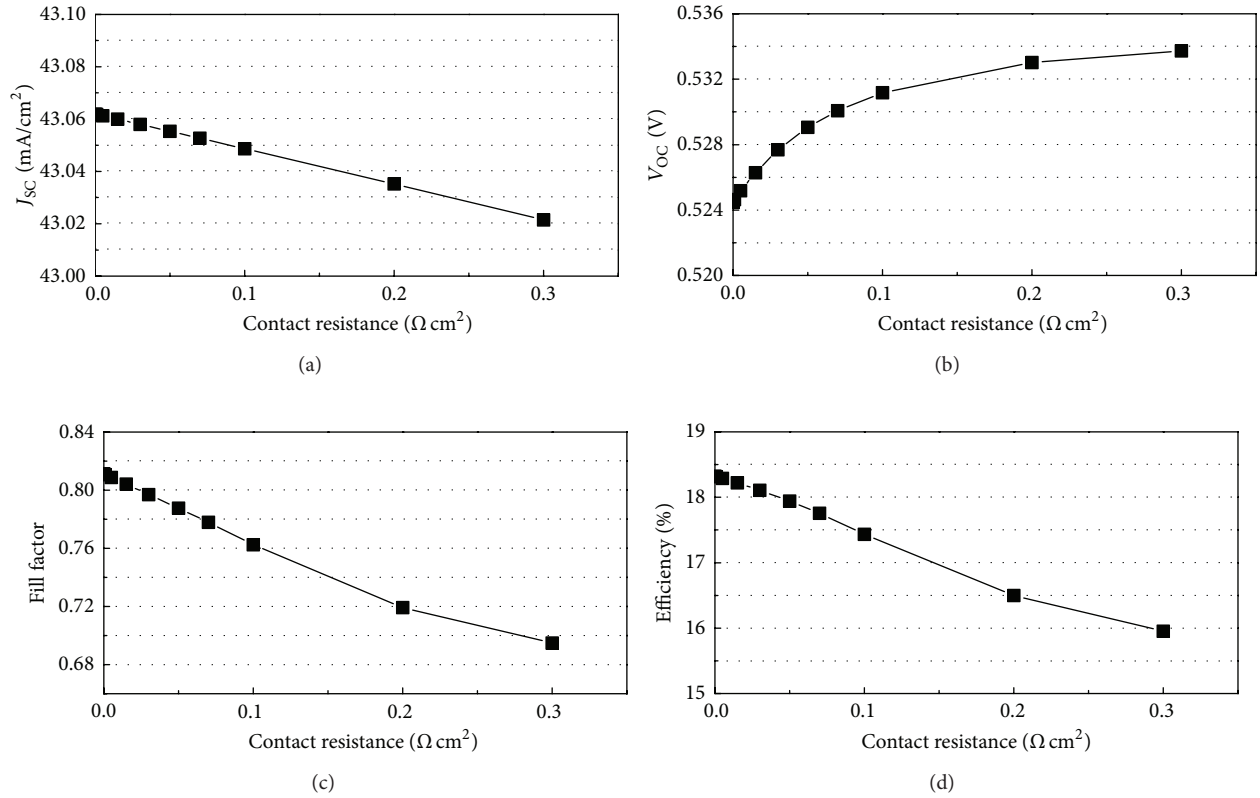

Figure 4: Dependence of the output parameters: (a) short circuit current density, (b) open circuit voltage, (c) fill factor, and (d) efficiency of the cell, on the contact resistance. The doping concentration of boron was set as 5×10^{18} atoms/cm^3.

contact resistance. Finally, the efficiency of the cell increased with the decrease of the contact resistance.

3.3. Dependence of Cell Parameters on N_B Including Contact Resistance. There are several factors determining the contact resistance of the crystalline silicon solar cell, such as the area and the quality of the metal electrode, the sheet resistance of the front surface of the cell, and the interface between the electrode and the silicon. Only the sheet resistance was considered to vary the contact resistance in this study. From the simulation, the sheet resistance of the n-type crystalline silicon wafer was identified along the doping concentration of boron, as shown in Figure 5. The contact resistance used in this simulation is shown in Table 1 [12].

Figure 6 shows the output parameters of the cell along the doping concentration of boron in the case of considering the effects of the contact resistance. The overall behaviors of J_{SC} and V_{OC} were nearly similar to the results of Figure 2. However, the fill factor of the cell, which did not vary in the doping concentration of $N_B > 5 \times 10^{17}$ atoms/cm^3 for zero contact resistance, slightly increased in that concentration range due to the decrease of contact resistance. This increase in the fill factor, with the increased doping concentration, affected the tendency in the final efficiency of solar cell. While the efficiency decreased at $N_B = 1 \times 10^{19}$ atoms/cm^3 for zero contact resistance, the lower contact resistance due to the higher doping concentration prevented the efficiency of the cell from decreasing up to $N_B = 1 \times 10^{20}$ atoms/cm^3. Finally, it was observed that, considering the contact resistance, the optimum doping concentration of boron for the n-type crystalline silicon solar cell was in the range of 1×10^{19}–1×10^{20} atoms/cm^3.

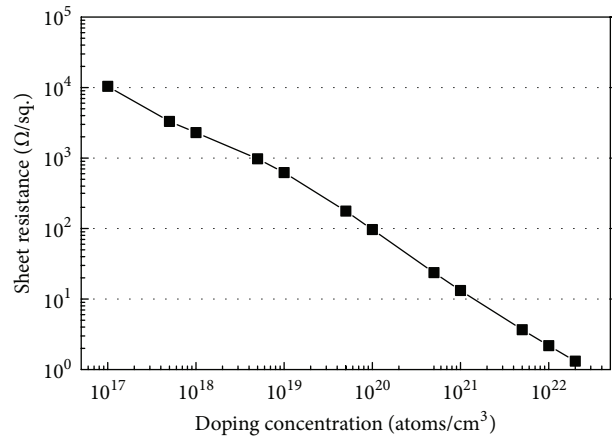

Figure 5: Dependence of the sheet resistance on the doping concentration of boron.

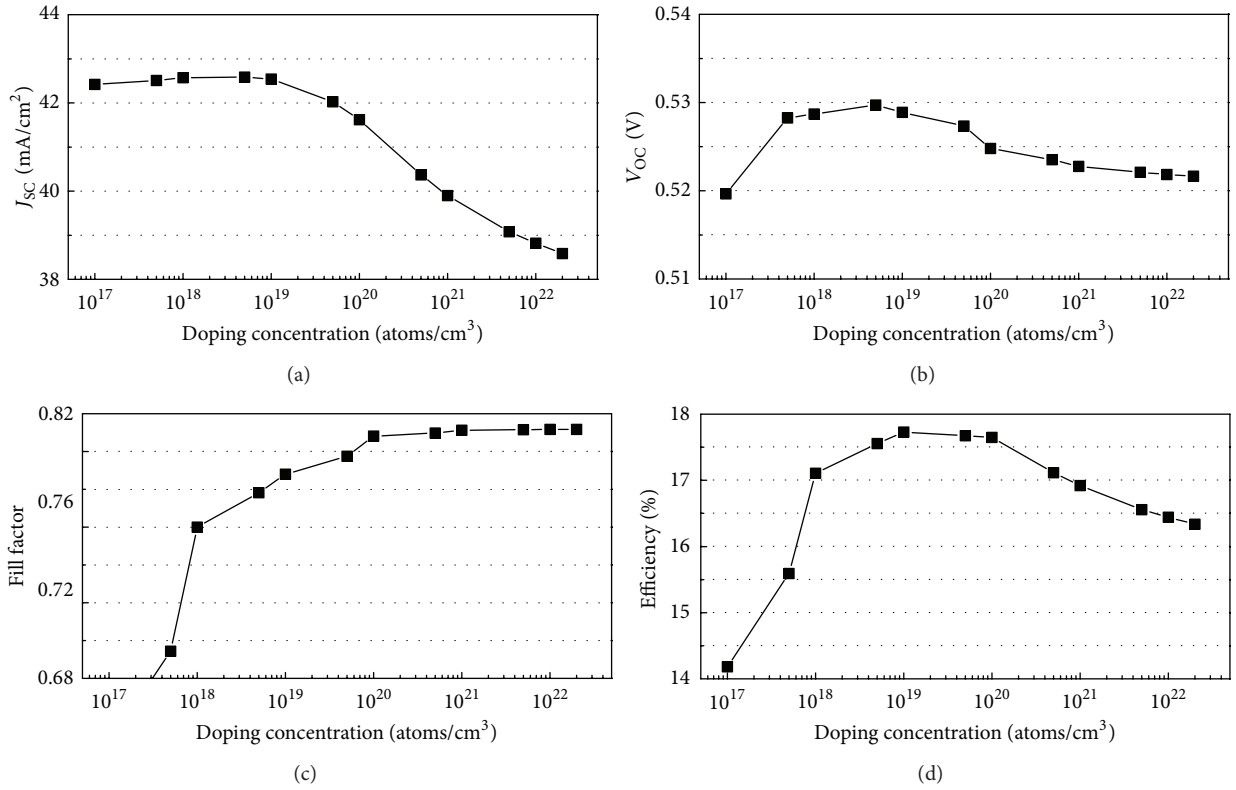

Figure 6: Dependence of the output parameters: (a) short circuit current density, (b) open circuit voltage, (c) fill factor, and (d) efficiency of the cell, on the boron concentration, including the effects of the contact resistance.

Table 1: Contact resistance at each doping concentration of boron.

Doping concentration (atoms/cm^3)	Contact resistance (Ωcm^2)
1×10^{17}	0.5
5×10^{17}	0.2
1×10^{18}	0.1
5×10^{18}	0.07
1×10^{19}	0.05
5×10^{19}	0.01
1×10^{20}	0.005
5×10^{20}	0.001
1×10^{21}	0.0005
5×10^{21}	0.0001
1×10^{22}	0.00001
2×10^{22}	0

4. Conclusion

In order to discover the optimized p^+ emitter for the n-type crystalline silicon solar cell, the boron-doped emitter was formed by the simulation method. The doping concentration of boron in the p^+ emitter was varied in the range of 1×10^{17}–2×10^{22} atoms/cm^3 to optimize the emitter structure. In the case that the contact resistance of the front metal electrode was assumed to be zero, the efficiency of the cell showed the maximum value at $N_B = 5 \times 10^{18}$–1×10^{19} atoms/cm^3. On the other hand, the nonzero contact resistance affected the performance of the solar cell. And with the increase of the contact resistance, which is closely related to the concentration of boron, the fill factor of the cell slightly decreased. Finally, the optimized doping concentration of boron was obtained in the range of 1×10^{19}–1×10^{20} atoms/cm^3.

Conflict of Interests

None of the authors have any conflict of interests with respect to the material contained in this paper.

Acknowledgments

This work was supported by the New & Renewable Energy Technology Development Program of the Korea Institute of Energy Technology Evaluation and Planning (KETEP) Grant funded by the Korea Government Ministry of Knowledge Economy (no. 20113010010140).

References

[1] M. A. Green, K. Emery, Y. Hishikawa, W. Warta, and E. D. Dunlop, "Solar cell efficiency tables," *Progress in Photovoltaics: Research and Applications*, vol. 19, no. 5, pp. 565–572, 2011.

[2] D. Macdonald and L. J. Geerligs, "Recombination activity of interstitial iron and other transition metal point defects in

p- and n-type crystalline silicon," *Applied Physics Letters*, vol. 85, no. 18, article 4061, 2004.

[3] F. W. Chen, T. T. A. Li, and J. E. Cotter, "Passivation of boron emitters on n-type silicon by plasma-enhanced chemical vapor deposited silicon nitride," *Applied Physics Letters*, vol. 88, no. 26, Article ID 263514, 2006.

[4] S. W. Glunz, S. Rein, J. Y. Lee, and W. Warta, "Minority carrier lifetime degradation in boron-doped Czochralski silicon," *Journal of Applied Physics*, vol. 90, no. 5, pp. 2397–2404, 2001.

[5] C. Schmiga, H. Nagel, and J. Schmidt, "19% efficient n-type Czochralski silicon solar cells with screen-printed aluminium-alloyed rear emitter," *Progress in Photovoltaics: Research and Applications*, vol. 14, no. 6, pp. 533–539, 2006.

[6] V. D. Mihailetchi, Y. Komatsu, G. Coletti et al., "High efficiency industrial screen printed n-type solar cells with front boron emitter," in *Proceedings of the 33rd IEEE Photovoltaic Specialists Conference*, San Diego, Calif, USA, 2008.

[7] F. Recart, I. Freire, L. Pérez, R. Lago-Aurrekoetxea, J. C. Jimeno, and G. Bueno, "Screen printed boron emitters for solar cells," *Solar Energy Materials and Solar Cells*, vol. 91, no. 10, pp. 897–902, 2007.

[8] J. Benick, B. Hoex, G. Dinggemans et al., "High-efficiency n-type silicon solar cells with front side boron emitter," in *Proceedings of the 24th European Photovoltaic Solar Energy Conference and Exhibition*, p. 863, Hamburg, Germany, 2009.

[9] D. Mathiot and J. C. Pfister, "Dopant diffusion in silicon: a consistent view involving nonequilibrium defects," *Journal of Applied Physics*, vol. 55, no. 10, pp. 3518–3530, 1984.

[10] *ATLAS User's Manual: Device Simulation Software*, Silvaco Inc., 2010.

[11] M. Bähr, S. Dauwe, L. Mittelstädt, J. Schmidt, and G. Gobsch, "Surface passivation and contact resistance on various emitters of screen-printed crystalline silicon solar cell," in *Proceedings of the 19th European Photovoltaic Solar Energy Conference and Exhibition*, p. 955, Paris, France, 2004.

[12] P. N. Vinod, "SEM and specific contact resistance analysis of screen-printed Ag contacts formed by fire-through process on the shallow emitters of silicon solar cell," *Journal of Materials Science: Materials in Electronics*, vol. 20, no. 10, pp. 1026–1032, 2009.